Overexpression in *Escherichia coli* and Functional Analysis of a Novel PP$_i$-Selective Porin, OprO, from *Pseudomonas aeruginosa*

ROBERT E. W. HANCOCK,[1] CHRISTINE EGLI,[1] ROLAND BENZ,[2] AND RICHARD J. SIEHNEL[1]*

Department of Microbiology, University of British Columbia, 300-6174 University Boulevard, Vancouver, British Columbia, Canada V6T 1Z3,[1] and Lehrstuhl für Biotechnologie, Universität Würzburg, D-8700 Würzburg, Germany[2]

Immediately upstream from and adjacent to the *oprP* gene, which codes for the phosphate-specific porin OprP of *Pseudomonas aeruginosa*, lies the PR region (*oprO*), which cross-hybridizes with *oprP* DNA. To determine the function of this region, the *oprO* gene was expressed behind the lactose promoter in *Escherichia coli*, and the resultant OprO protein was purified and reconstituted into planar lipid bilayers. OprO formed sodium dodecyl sulfate-stable trimers, cross-reacted immunologically with OprP, and, like OprP, formed an anion-specific, phosphate-selective porin. However, it demonstrated lower affinity for and higher maximal conductance of both chloride and phosphate than did the OprP channel. Examination by macroscopic conductance inhibition experiments of the affinity of OprO for phosphates of different lengths revealed a preference for PP$_i$ and tripolyphosphate over P$_i$, suggesting that OprO functioned as a PP$_i$-selective polyphosphate channel, in contrast to OprP, which has a marked preference for P$_i$.

The high-affinity phosphate transport system of *Pseudomonas aeruginosa* contains a number of inducible genes which are expressed when cells are starved for phosphate (17). Several of these components are analogous to the phosphate-starvation-inducible phosphate transport system components in *Escherichia coli* (6, 17). However, the phosphate-starvation-inducible outer membrane porin OprP of *P. aeruginosa* is both structurally (13, 15) and functionally (1, 7) distinct from the equivalent *E. coli* porin PhoE. In the course of cloning the *oprP* gene, we discovered that there was a linked region of DNA homology upstream of the *oprP* coding sequence (16). Indeed, this region (originally termed PR but renamed *oprO* here) hybridized to the *oprP* gene and to an oligonucleotide probe constructed on the basis of the amino-terminal amino acid sequence of the OprP protein (16). Furthermore, a fusion protein, constructed by fusing part of the *oprO* region to the *lacZ* amino terminus in plasmid pUC8, was able to cross-react with antiserum against monomeric, sodium dodecyl sulfate (SDS)-denatured OprP (16). However, there was no evidence obtained that the *oprO* region contained a gene or that the homology was extensive as opposed to localized. Indeed, there were substantial differences in the restriction patterns of *oprO* and *oprP*. In this paper, we have separately cloned the *oprO* and *oprP* genes into the expression vector pMMB66HE (11) and demonstrated that we can express, in *E. coli*, substantial amounts of proteins with similar molecular weights. To obtain information about the possible role and/or regulation of the *oprO* gene product, we have purified and characterized the OprO protein in detail in model membrane systems. The results obtained suggest that despite the substantial differences in the restriction patterns of *oprO* and *oprP*, these genes encode related proteins with distinct properties.

MATERIALS AND METHODS

Bacterial strains and media. *E. coli* K-12 strain CE1194 [F⁻ *thr leu proA2* Δ(*proA-phoE-gpt*) *his thi argE lacY galK xyl rpsL phoS21*] was utilized as the strain for cloning.

Plasmid pRS-XP, an 8.4-kb *Xho*I fragment of *P. aeruginosa* PAO1 chromosomal DNA ligated into the *Sal*I site of pUC18 (16, 20), was the source of the *oprP* and *oprO* genes. Plasmid pRSO-15 was constructed by sequentially cloning the small upstream *Hind*III-*Eco*RI fragment of *oprO* into plasmid pMMB66HE (11) and then ligating the larger downstream *Eco*RI fragment into the *Eco*RI site (Fig. 1). A similar two-step method was utilized to construct plasmid pRSP-3, which codes for OprP. Since expression of OprP was not seen with clones that interrupted regulatory sequences of *oprP* at the upstream *Hind*III site (data not shown), the 4.3-kb *Eco*RI fragment of pRS-XP (containing 94% of the mature OprP gene) was ligated to the leader peptide and first 25 amino acids of OprO at the *Eco*RI site to create pRSP-3 (Fig. 1). The N-terminal 25 amino acids of the mature OprO protein are identical to those encoded by the *oprP* gene (14). pRSP-3, therefore, codes for and expresses mature OprP. For expression studies, pRSO-15, pRSP-3, or the vector pMMB66HE was transformed into *E. coli* CE1248 (F⁻ *recA-56 phoE proA,B phoR-69 ompB-471* [= *ompR*] *thr leu thi pyrF thy ilvA his lacY argG tonA rpsL cod dra utr glpR*) (18), a strain with mutations preventing the production of porins OmpF, OmpC (because of the *ompB* mutation), and PhoE and constitutive for the *pho* regulon. For these studies, strain CE1248, containing one of the above plasmids, was grown on minimal medium (17) or LB medium containing 0.4% glucose (to repress porin LamB) and 75 μg of ampicillin per ml.

DNA procedures. Standard recombinant DNA procedures were performed as described by Maniatis et al. (9).

SDS-polyacrylamide gel electrophoresis, Western immunoblotting, and cell fractionation. SDS-polyacrylamide gel electrophoresis was performed as described previously (8) by using a 11% (wt/vol) acrylamide running gel. The Western immunoblot procedure utilized has been described previously (13). Antibodies to the trimer and monomer forms of OprP were raised in New Zealand White rabbits and purified according to the protocols described elsewhere (15).

Outer membrane preparations were constructed as described previously (5). Outer membranes were fractionated by resuspending them in 2% SDS–10 mM Tris-HCl (pH 7.4)
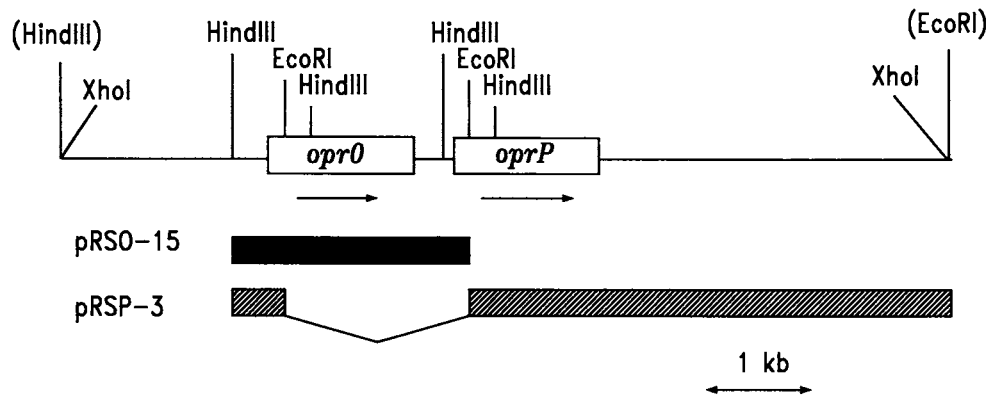
---

* Corresponding author.

FIG. 1. Restriction endonuclease map of the chromosomal DNA surrounding the *oprO* and *oprP* genes. Plasmid pRSO-15 contains the DNA represented above the solid black bar cloned into the expression vector pMMB66HE (10). Plasmid pRSP-3 contains the DNA represented above the hatched bars (fused at the *Eco*RI sites joined by the thin line) cloned into pMMB66HE. Note that the sequence of the *oprO* gene encoding the mature N terminus up to the *Eco*RI site is identical to that of the *oprP* gene (see text). Thus, pRSP-3 encodes mature OprP. Restriction sites in parentheses are derived from cloning vector pUC18 and are not chromosomally located.

and were pelleted for 1 h at 186,000 × g. The pellet was then resuspended in the same buffer plus 10 mM EDTA and pelleted as before. To prepare purified, gel-eluted preparations of porins OprO and OprP and of the CE1248 porin, the pellets were suspended in solubilization-reduction mix (8) without heating and were then subjected to SDS-polyacrylamide gel electrophoresis by using an 11% acrylamide gel. The trimeric form of OprP or OprO (revealed by staining a test strip) was then excised from the gel and eluted into H_2O. Some of the properties of OprO were confirmed by using protein purified from *P. aeruginosa* (14).

Lipid bilayer techniques. All lipid bilayer methods were performed exactly as described previously (2, 7).

RESULTS

Characterization of the porin activities in *E. coli* CE1248. Strain CE1248 was constructed by Van der Ley et al. (18) in such a manner that it lacked the major *E. coli* porins OmpF, OmpC, and PhoE. In addition, it was grown by us in glucose-containing medium to suppress production of LamB and had not undergone any obvious reversion event, as evidenced by the absence of a major porin band (Fig. 2, lane 3). Nevertheless, we considered the possibility that it still contained a minor porin activity with the potential to contaminate our OprP and OprO preparations. As a control experiment, this porin activity was purified from strain CE1248 by the technique described in Materials and Methods. Both partly purified and eluted preparations contained a single heat-modifiable band that ran on SDS-polyacrylamide gels at a monomer molecular weight of 37,000 after solubilization at 100°C for 10 min (Fig. 2, lane 6) and an oligomer (presumably a trimer) with an apparent molecular weight of 69,000 after solubilization at 25°C for 10 min (Fig. 2, lane 9).

The addition of this oligomeric porin to the aqueous salt solutions bathing a lipid bilayer membrane resulted in step-wise increases in conductance that were interpreted according to convention as the incorporation of single-channel-forming units into the membrane. Histograms of these conductance increases demonstrated a single peak, suggesting, in agreement with SDS gels, the presence of a single porin (data not shown). The average single-channel conductance, G, was calculated for a variety of salt solutions (Table 1). The conductance through the channel in the presence of

1 M KCl was substantially larger than that observed for all other well-characterized *E. coli* porins, including OmpF, OmpC, PhoE, K, LamB, and NmpC (3), although it was similar to the conductance of an uncharacterized channel that contaminated early LamB preparations (4). Lowering the salt concentration 10-fold led to a 10-fold lowering of conductance, suggesting the presence of large weakly selective aqueous channels. Varying the salt solution by increasing the size of the anion (to CH_3COO^-) or cation (to Li^+) suggested a preference for cations over anions. This observation was confirmed by zero current membrane potential measurement solved according to the Goldman-Hodgkin-Katz equation, by which it was determined that the permeability of K^+ through the CE1248 porin channel averaged 12.5-fold that of Cl^-. We concluded that this was a novel *E.*
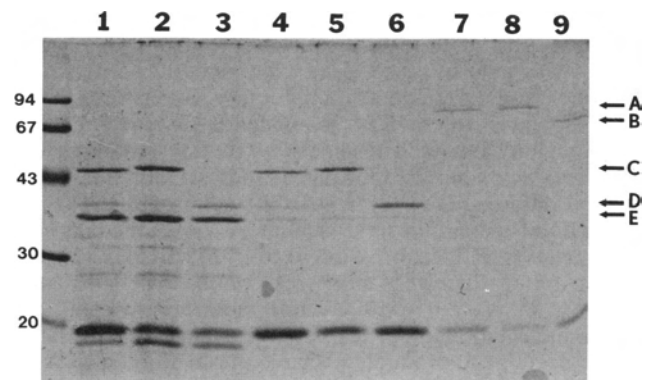

FIG. 2. SDS-polyacrylamide gel of outer membrane fractions from *E. coli* strains CE1248(pRSP-3) (lanes 1, 4, and 7), CE1248(pRSO-15) (lanes 2, 5, and 8), and CE1248(pMMB66HE) (lanes 3, 6, and 9). Lanes 1, 2, and 3, outer membrane fractions heated to 100°C for 10 min; lanes 4, 5, and 6, 2% SDS-insoluble outer membrane fractions heated to 100°C for 10 min; lanes 7, 8, and 9, 2% SDS-insoluble outer membrane fractions heated to 37°C for 10 min. Lanes 1, 2, and 3 were loaded with 20 μg of proteins, and lanes 4 to 9 were standardized to this starting level of protein and contain about 8 μg of protein. Molecular mass markers are given in kilodaltons. Letters indicate positions of the following proteins: A, OprP and OprO oligomers; B, CE1248 porin oligomer; C, OprP and OprO monomers; D, CE1248 porin monomer; E, OmpA.

TABLE 1. Average single-channel conductance (*G*) of *E. coli* CE1248 porin in different salt solutions[a]

Aqueous salt solution	Concn (M)	*G* (nS)	*n*
KCl	1	2.46	167
	0.1	0.23	111
$K^+CH_3COO^-$	1	2.04	70
LiCl	1	1.65	79
$Tris^+Cl^-$	1	0.44	126

[a] Membranes were formed from 1% diphytanoyl phosphatidyl choline in *n*-decane at a temperature of 25°C and an applied voltage of 20 mV. The pH of the aqueous solutions was 6 to 7. *G* was calculated as the average step increase in conductance in nanosiemens (nS). *n*, number of step increases in conductance that were recorded.
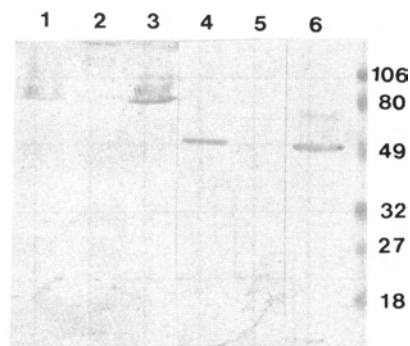

FIG. 3. Antigenic relationship of OprO to OprP. Shown are Western immunoblots of isolated *E. coli* outer membranes after separation on and transfer from an SDS-polyacrylamide gel. Lanes 1 and 4, outer membranes, containing OprO, from CE1248(pRSO-15); lanes 2 and 5, control outer membranes from CE1248 (pMMB66HE); lanes 3 and 6, outer membranes, containing OprP, from CE1248(pRSP-3). Lanes 1, 2, and 3 were reacted with polyclonal antibodies specific for OprP trimers (12); lanes 4, 5, and 6 were heated to 100°C for 10 min prior to loading and were reacted with polyclonal antibodies specific for OprP monomers (12). Prestained molecular mass markers are given in kilodaltons.

coli channel differing from other known porins in channel properties (3), although it could be similar to proteins Lc produced by lamboid phages PA-2 and HK253*hrk* (5, 19) or to the porinlike OmpG protein produced in *E. coli cog* mutants (10).

The CE1248 porin was present to a small extent in some of our OprO and OprP preparations, although in most of the lipid bilayer experiments described below it represented less than 5% of the observed channels and its properties allowed it to be easily differentiated from the OprP and OprO channels.

Overexpression of OprO and OprP in *E. coli* CE1248. The OprO-coding region (14) was cloned directly into the expression vector pMMB66HE to create plasmid pRSO-15. Since direct cloning of the *oprP* gene did not result in gene expression, we fused to the *oprP* gene the region of *oprO* encoding the leader sequence and the first 25 amino acids. This created in plasmid pRSP-3 a coding sequence which produced a mature OprP protein with the same amino acid sequence as that of authentic OprP (data not shown). These plasmids were transformed into *E. coli* CE1248. Growth of CE1248(pRSP-3) on minimal medium with glucose as a carbon source and isopropyl-β-D-thiogalactopyranoside (IPTG) to induce high expression of the *tac* promoter adjacent to the OprP gene resulted in expression of OprP in the *E. coli* outer membrane to a level almost equivalent of that of the *E. coli* major outer membrane protein OmpA (Fig. 2, lane 1). Similarly, growth of *E. coli* CE1248(pRSO-15) in the above medium resulted in high-level expression in the *E. coli* outer membrane of a protein, OprO, of slightly higher apparent molecular weight (50,000) than that of OprP (48,000) (Fig. 2; cf. lanes 1 and 2). When produced in *E. coli*, both OprP and OprO ran as oligomers (known to be trimers in the case of OprP [15]) of similar apparent molecular weights (82,000) (Fig. 2, lanes 7 and 8). The monomeric forms of OprP and OprO reacted on Western immunoblots with serum specific for OprP monomers, whereas the oligomers reacted with OprP trimer-specific serum (Fig. 3). Upon partial purification, or elution from gels, of the trimer forms, OprP and OprO retained the properties described above.

Function of OprO. The addition of small amounts (<100 ng) of partly purified or purified OprO protein to the aqueous salt solutions bathing lipid bilayer membranes resulted in the incorporation of channels into the membrane in a stepwise fashion (Fig. 4). The magnitudes of these channels were quite similar, with over 80% of the channels in most experiments being of the same size (Fig. 5). The single-channel conductance of 610 pS in 1 M KCl (Table 2) was less than 25% of that of the *E. coli* CE1248 porin and was easily

distinguished from the conductances of other *E. coli* porins (3, 4) or of the OprP porin, as described previously and confirmed in this study by using OprP purified from strain CE1248(pRSP-3) (2, 7). The single-channel conductance of OprO was little affected by changing the size of the cation in the aqueous salt solution. Indeed, the slightly lower conductance in 1 M $Tris^+Cl^-$ could be accounted for by the decreased ion activity in this solution. In contrast, increasing the size of the anions while keeping K^+ as the cation resulted in a steady decrease in the single-channel conductance (Fig. 6). With the exception of fluoride, there was a semilogarithmic relationship between the unhydrated radii of the ions and the average single-channel conductance, *G*. This suggested that the OprO channel was strongly anion selective and that it might actually contain an anion-binding site capable of stripping water molecules from these anions. The deviation of fluoride from the semilogarithmic relationship observed in Fig. 6 could relate to the relatively high hydration energy and consequent greater energy required to remove water molecules from fluoride ions prior to binding to the putative anion-binding site.

To confirm the presence of an anion-binding site in OprO, the average single-channel conductance in KCl solutions ranging in concentration from 0.03 to 3 M was measured. Results demonstrated saturation of the channel with increasing salt concentration, a result consistent with an anion-binding site. Replotting the data as an Eadie-Hofstee plot (Fig. 7) revealed an apparent K_s of 1.2 M and a maximal conductance, G_{max}, of 1,470 pS.

The above data were consistent with an anion-specific channel but did not reveal a preference of the channel for binding one anion over another. Therefore, inhibition experiments were pursued to see whether the channel was selective for a particular ion. Single-channel conductance experiments were performed with 0.3 M KCl solutions until about 10 to 20 channels had been observed to enter the membrane. The addition of potassium citrate or potassium acetate to a final concentration of 16 to 50 mM led to no change in conductance. However, the addition of potassium phosphate (pH 6.8 or 9.0) to a final concentration of 25 or 50 mM
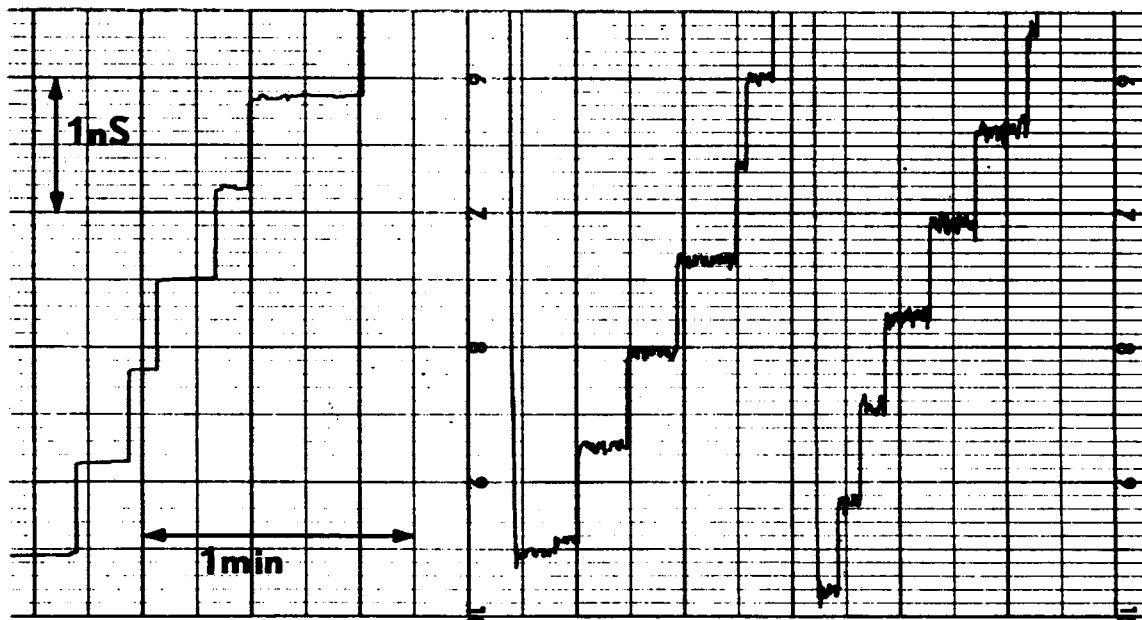
FIG. 4. Chart recording of single-channel conductance events due to incorporation of OprO channels into diphytanoylphosphatidyl choline bilayer membranes. The recording starts on the left, with the zero having been reset twice in the recording. Conditions of the experiment were as follows: salt solution, 1 M KCl; voltage applied, 20 mV; OprO concentration, 50 ng/ml; temperature, 25°C.

consistently resulted in a steep decrease in conductance followed by extremely unstable traces, suggesting rapid switching of channels from phosphate conducting to chloride conducting and back. To characterize this in more detail, macroscopic conductance inhibition studies were performed as described previously for OprP (7). Titration of increasing amounts of potassium phosphate (pH 6.8) into the aqueous 0.3 M KCl solutions bathing bilayers containing at least 100 OprO channels resulted in progressively decreasing conductance as a function of increasing phosphate concentrations. Data from three independent experiments were utilized as described previously (7) to calculate an I_{50} value, i.e., a concentration of phosphate resulting in 50% inhibition of chloride flux through the channel. These data revealed that

OprO contained a phosphate-binding site with an I_{50} of 2 mM (Table 3). However, analogous experiments with PP_i and tripolyphosphate revealed lower I_{50} values for both and an overall preference for PP_i.

DISCUSSION

The *oprO* region was previously identified as a region homologous to the *oprP* gene, which encodes the well-characterized phosphate porin OprP (15, 16). Thus, these genes cross-hybridized, contained an identically spaced triad of restriction sites at the putative amino termini, and, when fused to the start of the *lacZ* gene in vector pUC8, produced immunologically cross-reactive proteins of similar size (16). However, these genes have certain clear differences. For example, a Tn*501* insertion into the *oprP* gene, which is
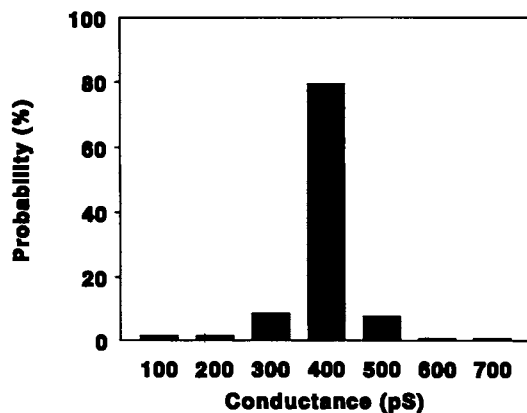

FIG. 5. Histogram of conductance increases due to incorporation of single molecules of OprO into diphytanoyl phosphatidyl choline membranes bathed by a 1 M KBr solution. The histogram represents 200 single-channel events from an experiment analogous to that of Fig. 4.

TABLE 2. Average single-channel conductance (G) of OprO and OprP in different 1 M salt solutions[a]

Aqueous salt solution	Anion radius[b] (nm)	G (pS)	
		OprO	OprP[b]
LiCl	0.181	643	223
KCl	0.181	610	238
Tris Cl	0.181	510	189
KF	0.133	728	415
KBr	0.195	395	223
KNO_3	0.198	191	94
KI	0.216	103	64
K_2HPO_4 (pH 6.8)	0.250	97	6

[a] Membranes were formed from 1% diphytanoyl phosphatidyl choline in *n*-decane at a temperature of 25°C and an applied voltage of 20 mV. The pH of the aqueous solutions was 6 to 7. G was calculated as the average step increase in conductance for at least 100 single events (except for KI, for which 45 events were measured). All aqueous salts were present at 1 M.

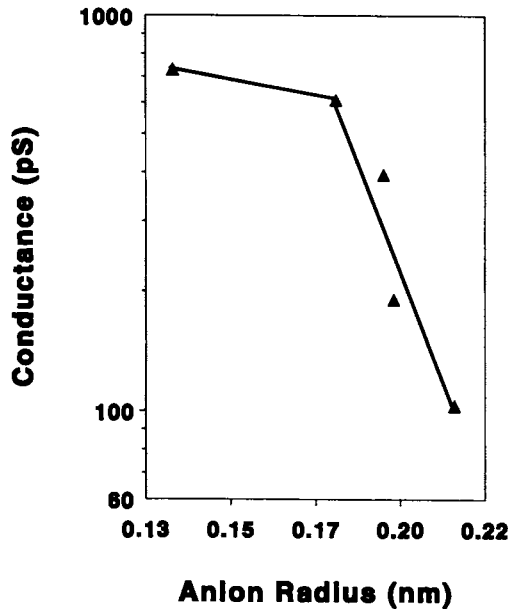[b] Anion radii and G values (= λ) for OprP were taken from references 2 and 7.

FIG. 6. Effect of anion size on conductance through OprO channel. Potassium salts (1 M) of (from left to right) F^-, Cl^-, Br^-, NO_3^-, and I^- were used. Data points represent the average single-channel conductances for 45 to 350 events in experiments analogous to that of Fig. 4.

downstream from the *oprO* gene (12), resulted in loss of OprP and an alteration in the kinetics of the phosphate-starvation-inducible (*Pst*) high-affinity phosphate uptake system. Polyclonal antisera, analogous to those utilized here, failed to reveal OprO in this OprP-deficient background. Therefore, to reveal the function of OprO and hence the possible regulatory mechanism of the *oprO* gene and product, we expressed this gene behind the *tac* promoter in *E. coli* and, after purification of OprO, investigated its function.

The data suggest that OprO has some similarities to OprP but also clear differences. For example, while both channels were anion specific, OprO had a 24-fold lower affinity and 5-fold higher maximal conductance for chloride than did
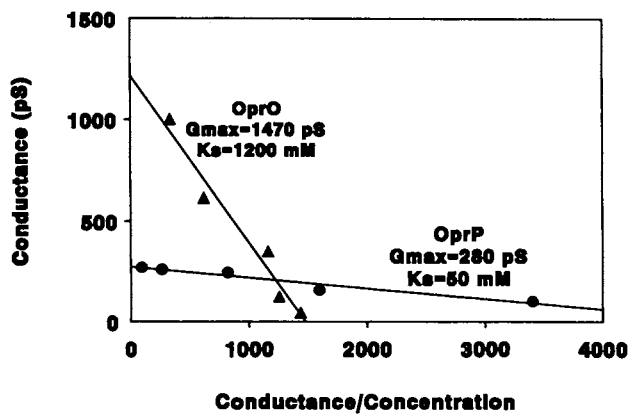

FIG. 7. Eadie-Hofstee plot of the influence of chloride concentration on conductance through OprP (taken from reference 2) and OprO. The maximal conductance (G_{max}) and stability constant of binding of chloride to the channel (K_s) were taken from the *y*-axis intercept and negative slope of these lines, respectively.

TABLE 3. Inhibition by phosphates of chloride conductance through the OprO and OprP channels

Anion[a]	I_{50} (mM)[b]	
	OprO	OprP
P_i	2.0	0.5
PP_i	0.3	4.9
Tripolyphosphate	1.5	—[c]

[a] Phosphate solutions were at pH 7.0.

[b] Concentration required to inhibit the flux of chloride through 100 or more channels by 50%. All macroscopic conductance inhibition experiments were performed at least three times. Because of the different affinities for chloride of OprO and OprP (Fig. 7), the chloride concentrations utilized were 300 and 30 mM, respectively. Data for OprP is taken from reference 7.

[c] No macroscopic conductance inhibition was observed, although membrane instability, due to the action of triphosphate on the diphytanoyl phosphatidyl choline bilayer, prevented the addition of more than about 1.2 mM triphosphate prior to membrane breakage.

OprP (Fig. 7). Similarly, OprO had a 4-fold lower affinity for P_i (Table 3) and a 16-fold higher maximal conductance (based on the conductance at 1 M phosphate; Table 2) than OprP. These data, and the influence of unhydrated anion size on conductance (Fig. 6), are most easily explained if the phosphate/anion binding site in OprO is similar in structure to that proposed for OprP, i.e., a triplet of symmetrically placed, positively charged lysine residues (each monomer of the porin trimer contributing one lysine) which coordinate the phosphate anion (which has a threefold symmetry of negative charges created by two negatively charged oxygens and one partly negatively charged oxygen in HPO_4^{2-} [7]). The lowered affinities and consequent higher maximal conductances of chloride and phosphate could be explained if the lysines were slightly further apart, creating a weaker cloud shell of shared electrons between the three lysines. This similarity in properties is consistent with the immunological cross-reactivity of the OprO and OprP gene products (Fig. 3) and the high degree of amino acid identity (71%), revealed by DNA sequencing (14), between OprP (GenBank accession number X53313) and OprO (to be submitted to GenBank Data Library).

The lower affinity for and higher maximal conductance of phosphate in the case of OprO was hard to understand, since OprO appeared to be more difficult to induce under phosphate starvation conditions in *P. aeruginosa*. Thus, an *oprP*::Tn501 mutant, grown into mid-logarithmic phase under conditions of phosphate deprivation, revealed no production of an immunologically cross-reacting protein (12). On the other hand, OprO was observed in such a background under conditions of overnight phosphate starvation, and there is a consensus Pho box in front of the *oprO* gene (14). Therefore, we looked for functional differences between OprO and OprP. We had previously demonstrated that PP_i bound to the OprP channel with considerably lower affinity than did P_i (7). This is explainable by the bend created by the oxygen linking the two phosphate atoms together in PP_i. However, we considered the possibility that this might not create as substantial a problem for the OprO channel, given the proposed greater spacing of the lysine residues in the phosphate-binding site. Surprisingly, however, PP_i bound with higher affinity to the OprO channel than did P_i (Table 3). Similarly, tripolyphosphate bound with higher affinity than P_i but with lower affinity than PP_i. Higher oligomers of phosphate were not tested because of problems with solubility and membrane stability. However, OprO bears the hallmarks of a polyphosphate channel. This is consistent

with the ability of *P. aeruginosa* to grow on polyphosphate as the sole source of phosphate and with the known high content in the environment of polyphosphate (a phosphate-storage compound for many organisms).

Previous mathematical modelling (2) demonstrated that the conductance properties of OprP could be explained by the hypothesis of two energy barriers and one binding site, and similar arguments are valid for OprO. However, one cannot distinguish between a two-barrier one-site model and a three-barrier two-site model by such mathematical modelling. Thus, there are at least two possible explanations for the enhanced affinity of OprO for PP_i over P_i. The first would suggest two binding sites placed in such a fashion as to take advantage of the PP_i molecule. A second would require that the geometry and distribution of charged amino acid residues in the OprO channel favored PP_i binding. Crystallization of both OprP, which is currently in progress, and OprO and/or site-directed mutagenesis of charged residues may help to distinguish between these possibilities.

ACKNOWLEDGMENTS

REFERENCES

1. Benz, R., R. P. Darveau, and R. E. W. Hancock. 1984. Outer membrane protein PhoE from *Escherichia coli* forms anion-selective pores in lipid bilayer membranes. Eur. J. Biochem. 140:319–324.
2. Benz, R., and R. E. W. Hancock. 1987. Mechanism of ion transport through the anion-selective channel of the *Pseudomonas aeruginosa* outer membrane. J. Gen. Physiol. 89:275–295.
3. Benz, R., A. Schmid, and R. E. W. Hancock. 1985. Ionic selectivity of gram-negative bacterial porins. J. Bacteriol. 162:722–727.
4. Benz, R., A. Schmid, T. Nakae, and G. H. Vos-Sheperkeuter. 1986. Pore formation by LamB of *Escherichia coli* in lipid bilayer membranes. J. Bacteriol. 165:978–986.
5. Blasband, A. J., W. R. Marcotte, and C. A. Schnaitman. 1986. Structures of the *lc* and *nmpC* outer membrane porin genes of lamboid bacteriophage. J. Biol. Chem. 261:12723–12732.
6. Filloux, A., M. Bally, C. Soscia, M. Murgier, and A. Lazdunski. 1988. Phosphate regulation in *Pseudomonas aeruginosa*: cloning of the alkaline phosphatase gene and identification of *phoB*- and *phoR*-like genes. Mol. Gen. Genet. 212:510–513.
7. Hancock, R. E. W., and R. Benz. 1986. Demonstration and

8. Hancock, R. E. W., and A. M. Carey. 1979. Outer membrane of *Pseudomonas aeruginosa*: heat- and 2-mercaptoethanol-modifiable proteins. J. Bacteriol. 140:902–910.
9. Maniatis, R., E. F. Fritsch, and J. Sambrook. 1982. Molecular cloning: a laboratory manual. Cold Spring Harbor Laboratory, Cold Spring Harbor, New York.
10. Misra, R., and S. A. Benson. 1989. A novel mutation, *cog*, which results in production of a new porin protein (OmpG) of *Escherichia coli* K-12. J. Bacteriol. 171:4105–4111.
11. Morales, V., M. M. Bagdasarian, and M. Bagdasarian. 1990. Promiscuous plasmids of the IncQ group: mode of replication and use for gene cloning in gram-negative bacteria, p. 229–241. *In* S. Silver, A. N. Chakrabarty, B. Iglewski, and S. Kaplan (ed.), *Pseudomonas*: biotransformations, pathogenesis, and evolving biotechnology. American Society for Microbiology, Washington, D.C.
12. Poole, K., and R. E. W. Hancock. 1986. Isolation of a *Tn501* insertion mutant lacking porin protein P of *Pseudomonas aeruginosa*. Mol. Gen. Genet. 202:403–409.
13. Poole, K., and R. E. W. Hancock. 1986. Phosphate-starvation-induced outer membrane proteins of members of the families *Enterobacteriaceae* and *Pseudomonodaceae*: demonstration of immunological cross-reactivity with an antiserum specific for porin protein P of *Pseudomonas aeruginosa*. J. Bacteriol. 165:987–993.
14. Siehnel, R., C. Egli, and R. E. W. Hancock. Unpublished data.
15. Siehnel, R., N. L. Martin, and R. E. W. Hancock. 1990. Sequence and relatedness in other bacteria of the *Pseudomonas aeruginosa oprP* gene coding for the phosphate specific porin P. Mol. Microbiol. 4:831–838.
16. Siehnel, R. J., E. A. Worobec, and R. E. W. Hancock. 1988. Cloning of the *Pseudomonas aeruginosa* outer membrane porin protein P gene: evidence for a linked region of DNA homology. J. Bacteriol. 170:2312–2318.
17. Siehnel, R. J., E. A. Worobec, and R. E. W. Hancock. 1988. Regulation of components of the *Pseudomonas aeruginosa* phosphate-starvation-inducible regulon in *Escherichia coli*. Mol. Microbiol. 2:347–352.
18. Van der Ley, P., H. Amesz, J. Tomassen, and B. Lugtenberg. 1985. Monoclonal antibodies directed against the cell surface-exposed part of PhoE pore protein of the *Escherichia coli* K-12 outer membrane. Eur. J. Biochem. 147:401–407.
19. Verhoef, C., R. Benz, A. P. W. Poon, and J. Tommassen. 1987. New pore protein produced in cells lysogenic for *Escherichia coli* phage HK253*hrk*. Eur. J. Biochem. 164:141–145.
20. Yanisch-Perron, C., J. Vieira, and J. Messing. 1985. Improved M13 phage cloning vectors and host strains: nucleotide sequences of the M13mp18 and pUC19 vectors. Gene 33:103–119.